
MACHINE LEARNING MODEL TO CLUSTER AND MAP TRIBOCORROSION REGIMES IN FEATURE SPACE

A PREPRINT

 **Rahul Ramachandran**

Department of Mechanical Engineering
University of Nevada, Reno
Reno, NV 89557
r.ramacha6@gmail.com

June 11, 2020

ABSTRACT

Tribocorrosion maps serve the purpose of identifying operating conditions for acceptable rate of degradation. This paper proposes a machine learning based approach to generate tribocorrosion maps, which can be used to predict tribosystem performance. First, unsupervised machine learning is used to identify and label clusters from tribocorrosion experimental data. The identified clusters are then used to train a support vector classification model. The trained SVM is used to generate tribocorrosion maps. The generated maps are compared with the standard maps from literature.

Keywords Machine learning · SVM · K-means clustering · Tribocorrosion maps

1 Introduction

Development and implementation of predictive models from experimental data using machine learning (ML) have been an active research topic in material science and engineering. In ML, a computer program based on an algorithm learns from historical data to improve a performance metric. The selection of the algorithm, and metric depends on the specific data and problem at hand. The commonly used ML algorithms can be divided into regression, probability estimation, classification and clustering [1]. Recently ML tools have been used in tribology to build predictive models for friction coefficient [2, 3], wear rate [4] and wear volume [5], to design lubricants [6–8] and functional materials [9], for tribocorrosion [10] and surface roughness [11] modeling, for wear particle classification [12], and in corrosion modeling [13–19].

The combined effect of wear and corrosion, known as tribocorrosion, is often undesirable and can result in accelerated material degradation. It is frequently encountered where surfaces are in contact with each other in a corrosive environment. This phenomenon is relevant to a range of industries from energy and transportation to healthcare. Interfacial conditions such as materials, lubrication, normal load, relative speed, surface topography, temperature, humidity, pH etc. can affect the degradation process. The total mass change by tribocorrosion (K_{wc}) can be explained using the analysis in [20] as

$$K_{wc} = K_w + K_c \quad (1)$$

where K_w is the total mass of material removed due to wear, K_c is the total mass of material removed due to corrosion. K_w is $K_{wo} + \Delta K_w$, where K_{wo} is the mass loss by wear in the absence of corrosion, and ΔK_w is the synergistic effect of corrosion on wear. K_c is $K_{co} + \Delta K_c$, where K_{co} is the mass loss by corrosion in the absence of wear, and ΔK_c is the additive effect (enhancement) of corrosion due to wear. These terms can be determined experimentally and

used to characterize the dominant degenerative mechanism for the tribosystem. Tribocorrosion regimes [21] are defined based on the ratio K_c/K_w as follows:

$$K_c/K_w \leq 0.1, \quad \text{wear} \quad (2)$$

$$0.1 < K_c/K_w \leq 1, \quad \text{wear-corrosion} \quad (3)$$

$$1 < K_c/K_w \leq 10, \quad \text{corrosion-wear} \quad (4)$$

$$K_c/K_w > 10, \quad \text{corrosion} \quad (5)$$

Tribocorrosion mechanism maps and synergy maps enable to illustrate these regimes as functions of interfacial conditions such as normal load, sliding speed, pH etc. These maps are helpful to identify conditions of minimal degradation, for process optimization, and in the design of functional materials and coatings [22].

The standard approach to create tribocorrosion maps involve extensive experiments to generate data, determination of the regimes, and creating graphical illustrations. Machine learning can be used to create accurate predictive models from the experimental data quickly and automatically. Although ML tools are widely used in tribology, no previous studies have dealt with identifying clusters and creating tribocorrosion maps using ML tools. This study uses both unsupervised and supervised learning techniques to make predictive models for tribocorrosion and to generate maps.

2 Proposed Approach

The predictive model is developed in two parts. The first part involves identifying clusters in tribocorrosion experimental data using the K Means clustering technique. The second part involves training a support vector classifier using the dataset and the cluster labels. The support vectors can then be used to draw wear-corrosion mechanism, synergy, and wastage maps. Two experimental datasets from published literature are used in this study. Dataset 1 is tribocorrosion data of Ti–25Nb–3Mo–3Zr–2Sn alloy in simulated Hank’s solution [23], and dataset 2 is tribocorrosion data of Co–Cr/UHMWPE couple in Ringer’s solution [24]. These materials are relevant because of their applications in the biomedical industry for manufacturing implants. It is essential to understand the degradation and predict lifecycle of implants under various conditions, both of which can possibly be done with ML. The data was standardized by removing the mean and scaling to unit variance before training the model. The models were developed using the open-source ML package scikit-learn [25].

2.1 Unsupervised learning

Clustering is a multivariate statistical technique used to group data into clusters based on their underlying structure. A commonly used technique is the K-means clustering. The number of clusters (K) and the starting centroids are provided as input parameters. This is followed by an iterative process of assigning the data points to each cluster based on their Euclidean squared distance to the corresponding centroid, and recalculating the centroids, until the centroids can no longer be adjusted.

In this study K-means clustering was used for exploratory analysis. For this, an unsupervised ML model was developed using the standardized datasets. In order to determine the optimal value of K for each dataset, the elbow method [26] and the silhouette coefficients [27] were used.

2.2 Supervised learning

Support Vector Machines (SVMs) [28] are supervised ML algorithms that can be used in classification and regression [29]. SVMs use kernel functions to map datapoints from an input space to a high dimensional feature space to establish linear decision boundaries (hyper planes). These boundaries become nonlinear when transformed back to original input space, thus making non-linear classification possible. The datapoints closest to the hyperplane are called support vectors. Four basic kernel functions $K(x_i, x_j)$ are linear (eq. 6), polynomial (eq. 7), radial basis function (RBF) (eq. 8) and sigmoid (eq. 9). The hyperparameters γ , r , and d associated with the SVMs are generally tuned using cross-validation or grid search [30].

$$K(x_i, x_j) = x_i^T x_j \quad (6)$$

$$K(x_i, x_j) = (\gamma x_i^T x_j + r)^d, \gamma > 0 \quad (7)$$

$$K(x_i, x_j) = e^{-\gamma \|x_i - x_j\|^2}, \gamma > 0 \quad (8)$$

$$K(x_i, x_j) = \tanh(\gamma x_i^T x_j + r), \gamma > 0 \quad (9)$$

The labelled datasets obtained after clustering is used to train SVM classification models. Since SVMs are designed for binary classification, different strategies can be adopted based on the multiclass classification problem at hand [31].

3 Results and Discussion

3.1 Identifying the clusters

Clustering was done for a range of K values based on the data, and the resulting within-cluster sum of squares (WCSS) was obtained. The red lines in Figures 1a and 1b show the WCSS for datasets 1 and 2 respectively. The elbow can be observed at K=3 in Figure 1a. However, the elbow in Figure 1b is not obvious. Further analysis was done by calculating the silhouette coefficients. The blue lines in Figures 1a and 1b show the silhouette coefficients for a range of K values for datasets 1 and 2 respectively. The best value of K is where the silhouette coefficient is maximum, which is equal to 3 for both the datasets.

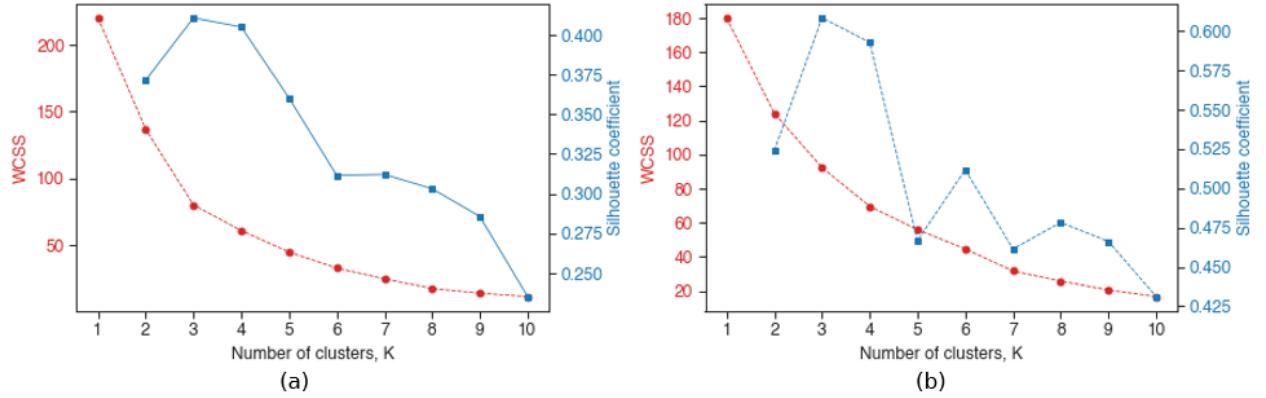


Figure 1: Metrics to determine the optimum number of clusters for (a) dataset 1 and (b) dataset 2. Within-cluster sum of squares (WCSS) is denoted by the red circles and dashed line. Silhouette coefficients are denoted by blue squares and solid line.

The two datasets were clustered and labelled using K-means clustering with K=3. The three clusters in dataset 1 can clearly be distinguished on a K_w versus K_c plot as shown in Figure 2a. The single datapoint that forms a distinct cluster is identified as the corrosion-wear cluster, as it has a high K_c compared to K_w . The other two clusters are closer to the K_w axis, denoting wear-corrosion synergy. The cluster near the origin is labelled as the low wear-corrosion synergy cluster, and the cluster on the right is labelled as the high wear-corrosion synergy cluster.

Similarly, the three clusters in dataset 2 can be clearly identified on a K_c versus K_w plot as shown in Figure 3a. The cluster with the very small values of K_c , and large values of K_w can be identified as having wear as the predominant degradation mechanism. The cluster with similar values of K_c and K_w can be identified as having corrosion-wear synergy. The third cluster approximately in the center of the plot, is classed as having wear-corrosion synergy. This classification is similar to the results obtained in the source [24].

3.2 Tribocorrosion maps

Since the two datasets under consideration have three clusters each, a one-vs-one strategy is used to train the SVM and perform classification. The clusters in dataset 1 were labelled 0, 1 and 2. The features used were abrasive concentration (g/cm^3) and normal load (N). A polynomial kernel function was chosen to map the datapoints to a higher dimensional space. Values for the hyperparameters in eq. 7 were as follows: kernel parameter $\gamma = 2$, penalty parameter = 10, degree $d = 2$ and $r = 0$. The model was trained on the labelled dataset. The tribocorrosion map (Figure 2b) of the feature space—abrasive particle concentration vs normal load—is generated by predicting using the trained model. The map shows the three previously identified clusters. From the map, the major degradation mechanism is identified as

wear-induced corrosion, which is similar to the results obtained by [23]. Corrosion-induced wear is the degradation mechanism for a small segment of the operating conditions.

Similarly, the clusters in dataset 2 were labelled as 0, 1 and 2. The features used were potential (V) and normal load (N). RBF kernel (eq. 8) was used to map the dataset 2 to a higher dimensional space. The model was trained on the labelled dataset with hyperparameter $\gamma = 7$ and the penalty parameter as 10. The tribocorrosion map obtained by predicting using the trained model on the feature space is shown in Figure 3b. The three degradation mechanisms—wear, wear-corrosion and corrosion-wear—are mapped on the potential vs normal load graph. The wear-corrosion cluster as identified in Figure 3a covers most of the area in the tribocorrosion map. Wear is dominant in the potential range -0.5 to -0.3 V. Corrosion-induced wear is dominant around potential of 0 V.

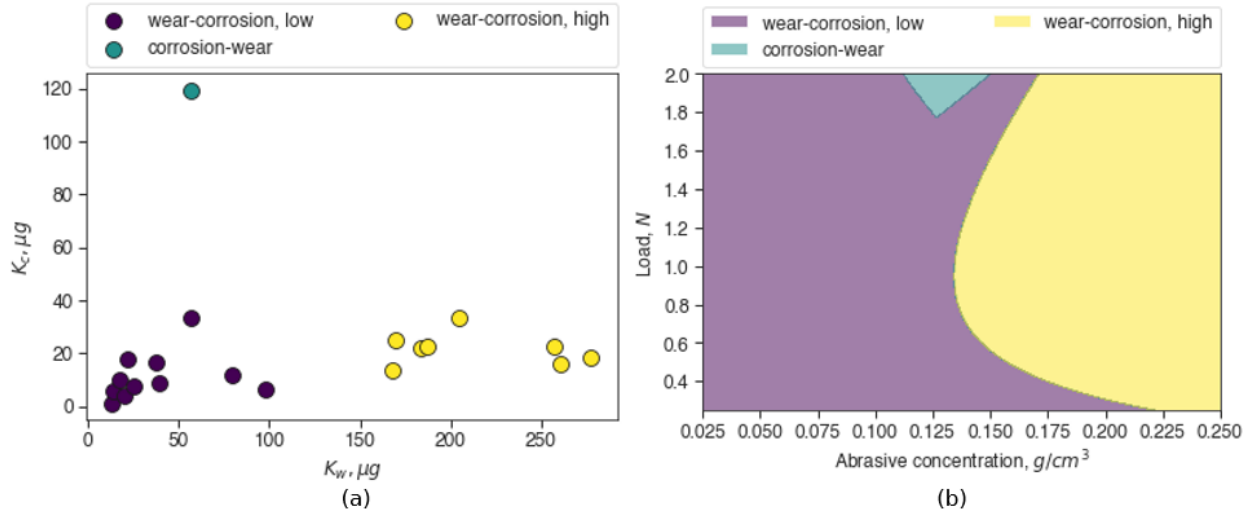


Figure 2: (a) Three clusters in dataset 1 identified using K-means clustering (b) tribocorrosion mechanism map using SVM for the titanium alloy.

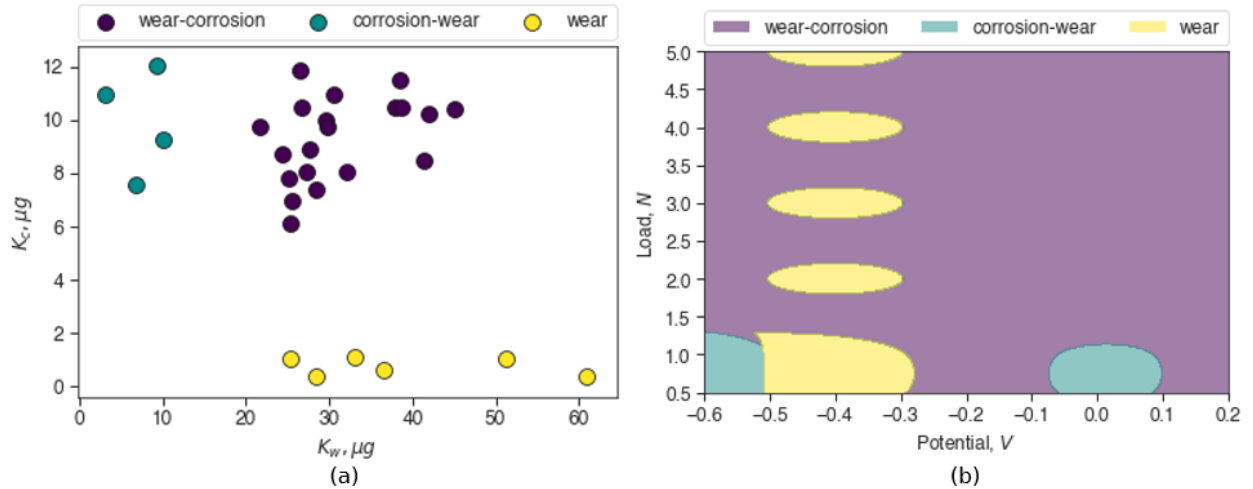


Figure 3: (a) Three clusters in dataset 2 identified using K-means clustering (b) tribocorrosion mechanism map of Co-Cr generated using SVM.

For the two tribosystems under consideration, the degradation mechanisms can be determined and thus an acceptable material loss rate can be maintained by controlling the interface conditions as per Figures 2b and 3b. Although the material data used in this study are from biomedical implant materials, the method proposed is relevant to applications such prediction of degradation mechanism, material selection, and lifecycle estimation of mining tools, automotive and marine machine components.

In this study the performance of the models was not evaluated using test and validation datasets due to limited sample sizes. Note that these are necessary to avoid over-fitting the models. In future work, more robust ML predictive models will be created using larger training dataset.

4 Conclusion

A machine learning based approach is proposed to generate tribocorrosion maps. First, tribocorrosion experimental data is clustered and labelled based on their underlying structure. The labelled datasets are used to train SVM classification models, with the labels being the targets. The problem being non-linear, RBF and polynomial kernels are used to map the data and establish the decision boundaries. The trained models are used to predict the targets on the feature space to generate the tribocorrosion maps. The tribocorrosion maps thus generated are relevant to applications such as material selection, identifying degradation mechanisms, and lifecycle estimation

References

- [1] Y. Liu, T. Zhao, W. Ju, and S. Shi, "Materials discovery and design using machine learning," *Journal of Materiomics*, vol. 3, no. 3, pp. 159–177, 2017.
- [2] L. A. Gyurova and K. Friedrich, "Artificial neural networks for predicting sliding friction and wear properties of polyphenylene sulfide composites," *Tribology International*, vol. 44, no. 5, pp. 603–609, 2011.
- [3] H. Xie, Z. Wang, N. Qin, W. Du, and L. Qian, "Prediction of Friction Coefficients During Scratch Based on an Integrated Finite Element and Artificial Neural Network Method," *Journal of Tribology*, vol. 142, oct 2019.
- [4] I. I. Argatov and Y. S. Chai, "An artificial neural network supported regression model for wear rate," *Tribology International*, vol. 138, pp. 211–214, 2019.
- [5] K. Velten, R. Reinicke, and K. Friedrich, "Wear volume prediction with artificial neural networks," *Tribology International*, vol. 33, no. 10, pp. 731–736, 2000.
- [6] S. Bhaumik, S. D. Pathak, S. Dey, and S. Datta, "Artificial intelligence based design of multiple friction modifiers dispersed castor oil and evaluating its tribological properties," *Tribology International*, vol. 140, p. 105813, 2019.
- [7] C. Humelnicu, S. Ciortan, and V. Amortila, "Artificial Neural Network-Based Analysis of the Tribological Behavior of Vegetable Oil–Diesel Fuel Mixtures," *Lubricants*, vol. 7, no. 4, 2019.
- [8] W. Rashmi, M. Osama, M. Khalid, A. K. Rasheed, S. Bhaumik, W. Y. Wong, S. Datta, and G. TCSM, "Tribological performance of nanographite-based metalworking fluid and parametric investigation using artificial neural network," *The International Journal of Advanced Manufacturing Technology*, vol. 104, no. 1, pp. 359–374, 2019.
- [9] A. Vinoth and S. Datta, "Design of the ultrahigh molecular weight polyethylene composites with multiple nanoparticles: An artificial intelligence approach," *Journal of Composite Materials*, vol. 54, no. 2, pp. 179–192, 2020.
- [10] P. Srinivasa Pai, M. T. Mathew, M. M. Stack, and L. A. Rocha, "Some thoughts on neural network modelling of microabrasion–corrosion processes," *Tribology International*, vol. 41, no. 7, pp. 672–681, 2008.
- [11] I. Buj-Corral, M. Sivatte-Adroer, and X. Llanas-Parra, "Adaptive indirect neural network model for roughness in honing processes," *Tribology International*, vol. 141, p. 105891, 2020.
- [12] Y. Peng, J. Cai, T. Wu, G. Cao, N. Kwok, S. Zhou, and Z. Peng, "A hybrid convolutional neural network for intelligent wear particle classification," *Tribology International*, vol. 138, pp. 166–173, 2019.
- [13] R. Chelariu, G. D. Suditu, D. Mareci, G. Bolat, N. Cimpoesu, F. Leon, and S. Curteanu, "Prediction of Corrosion Resistance of Some Dental Metallic Materials with an Adaptive Regression Model," *JOM*, vol. 67, no. 4, pp. 767–774, 2015.
- [14] J.-S. Chou, N.-T. Ngo, and W. K. Chong, "The use of artificial intelligence combiners for modeling steel pitting risk and corrosion rate," *Engineering Applications of Artificial Intelligence*, vol. 65, pp. 471–483, 2017.
- [15] M. J. Jiménez-Come, I. J. Turias, J. J. Ruiz-Aguilar, and F. J. Trujillo, "Characterization of pitting corrosion of stainless steel using artificial neural networks," *Materials and Corrosion*, vol. 66, no. 10, pp. 1084–1091, 2015.
- [16] M. Kamrunnahar and M. Urquidi-Macdonald, "Prediction of corrosion behavior using neural network as a data mining tool," *Corrosion Science*, vol. 52, pp. 669–677, mar 2010.

- [17] D. Mareci, E.-N. Dragoi, G. Bolat, R. Chelariu, D. Gordin, and S. Curteanu, "Modelling the influence of pH, fluoride, and caffeine on the corrosion resistance of TiMo alloys by artificial neural networks developed with differential evolution algorithm," *Materials and Corrosion*, vol. 66, no. 9, pp. 982–994, 2015.
- [18] D. Mareci, G. D. Suditu, R. Chelariu, L. C. Trincă, and S. Curteanu, "Prediction of corrosion resistance of some dental metallic materials applying artificial neural networks," *Materials and Corrosion*, vol. 67, no. 11, pp. 1213–1219, 2016.
- [19] K. Xu, A. R. Luxmoore, and F. Deravi, "Comparison of shape features for the classification of wear particles," *Engineering Applications of Artificial Intelligence*, vol. 10, no. 5, pp. 485–493, 1997.
- [20] Z. Yue, P. Zhou, and J. Shi, "Some Factors Influencing Corrosion-Erosion Performance of Materials," in *Proceedings of conference on wear of materials* (K. C. Luedema, ed.), (New York), pp. 763–770, ASME, 1987.
- [21] M. M. Stack, S. Zhou, and R. C. Newman, "Effects of particle velocity and applied potential on erosion of mild steel in carbonate/bicarbonate slurry," *Materials Science and Technology*, vol. 12, no. 3, pp. 261–268, 1996.
- [22] R. J. K. Wood, "Tribo-corrosion of coatings: a review," *Journal of Physics D: Applied Physics*, vol. 40, pp. 5502–5521, aug 2007.
- [23] Z. Wang, Y. Li, W. Huang, X. Chen, and H. He, "Micro-abrasion–corrosion behaviour of a biomedical Ti–25Nb–3Mo–3Zr–2Sn alloy in simulated physiological fluid," *Journal of the Mechanical Behavior of Biomedical Materials*, vol. 63, pp. 361–374, 2016.
- [24] M. M. Stack, J. Rodling, M. T. Mathew, H. Jawan, W. Huang, G. Park, and C. Hodge, "Micro-abrasion–corrosion of a Co–Cr/UHMWPE couple in Ringer’s solution: An approach to construction of mechanism and synergism maps for application to bio-implants," *Wear*, vol. 269, no. 5, pp. 376–382, 2010.
- [25] F. Pedregosa, G. Varoquaux, A. Gramfort, V. Michel, B. Thirion, O. Grisel, M. Blondel, P. Prettenhofer, R. Weiss, V. Dubourg, J. Vanderplas, A. Passos, D. Cournapeau, M. Brucher, M. Perrot, and E. Duchesnay, "Scikit-learn: Machine learning in Python," *Journal of Machine Learning Research*, vol. 12, pp. 2825–2830, 2011.
- [26] G. W. Milligan and M. C. Cooper, "An examination of procedures for determining the number of clusters in a data set," *Psychometrika*, vol. 50, no. 2, pp. 159–179, 1985.
- [27] P. J. Rousseeuw, "Silhouettes: A graphical aid to the interpretation and validation of cluster analysis," *Journal of Computational and Applied Mathematics*, vol. 20, pp. 53–65, 1987.
- [28] C. Cortes and V. Vapnik, "Support-vector networks," *Machine Learning*, vol. 20, no. 3, pp. 273–297, 1995.
- [29] S. Raghavendra. N and P. C. Deka, "Support vector machine applications in the field of hydrology: A review," *Applied Soft Computing*, vol. 19, pp. 372–386, 2014.
- [30] C.-W. Hsu, C.-C. Chang, and C.-J. Lin, "A Practical Guide to Support Vector Classification," tech. rep., Department of Computer Science, National Taiwan University, 2003.
- [31] J. Brownlee, "How to Use One-vs-Rest and One-vs-One for Multi-Class Classification." <https://machinelearningmastery.com/one-vs-rest-and-one-vs-one-for-multi-class-classification/>, 2020 (accessed June 1, 2020).